Evaluation of the Accuracy of Photogrammetric Reconstruction of Bathymetry Using Differential GNSS Synchronized with an Underwater Camera

Eric Lo [1], Hilda Lozano Bravo [1], Nathan Hui [1], Erica Nocerino [2], Fabio Menna [3], Dominique Rissolo[1], Falko Kuester [1]

[1] Cultural Heritage Engineering Initiative, University of California, San Diego, USA – (eklo, hlozanobravo, nthui, drissolo, fkuester)@ucsd.edu
[2] Department of Humanities and Social Sciences, University of Sassari, Sassari, Italy – enocerino@uniss.it
[3] Department of Chemical, Physical, Mathematical and Natural Sciences, University of Sassari, Sassari, Italy - fmenna@uniss.it

Keywords: Underwater photogrammetry, PPK GNSS, Bathymetry, 3D model, Accuracy.

Abstract

Photogrammetry is a valuable tool for 3D documentation, mapping, and monitoring of underwater environments. However, the ground control surveys necessary for georeferencing and validation of the reconstructed bathymetry are difficult and time consuming to perform underwater, and thus impractical to scale to larger areas. Underwater direct georeferencing, using a differential GNSS receiver synchronized with an underwater camera system, offers an attractive alternative to surveying underwater ground control points in conditions when the seafloor is clearly visible from the surface. In this paper, the design of an underwater direct georeferencing system using mostly commercial off the shelf components is presented. The accuracy of the system is evaluated against geodetic survey based on trilateration and leveling, as well as by RTK (real time kinematic) positioning using a tilt-compensated GNSS receiver mounted on an extended pole to allow measurements of points in up to 7 m in water depth. Tests were conducted in a controlled outdoor pool setting with depths from 1-3 m, as well as in a 10 m x 10 m test plot established on the seafloor in a near-shore environment by Catalina Island, California at depths from 4-10 m. Comparing the geometry of the photogrammetric reconstruction with the geodetic survey yielded sub centimeter consistency, and 1 mm accuracy in length measurement was achieved when compared with calibrated 0.5 m scale bars. Through repeated surveys of the same area, repeatability of georeferencing is demonstrated within expectations for differential GNSS positioning, with horizontal errors at sub centimeter level, and vertical errors of up to 3 cm in the worst cases. These tests demonstrate the benefits of the underwater direct georeferencing approach in shallow waters, which can be scaled up much more easily than measuring underwater ground control points with traditional approaches, making this an ideal option for collecting accurate bathymetry of the seafloor over large coastal areas with clear waters.

1. Introduction

Photogrammetry is a powerful technique for 3D reconstruction. However, deformations in the photogrammetric model may occur if proper self-calibration procedures and camera network geometries are not implemented. Traditionally, constraints can be provided by ground control points with accurately known coordinates of suitable accuracy distributed throughout the survey area (James and Robson, 2014; Nocerino et al., 2014). In terrestrial and aerial photogrammetry, the ground control survey can be achieved using a total station or by directly measuring the position of the points with GNSS receivers, depending on the required accuracy. Alternatively, direct georeferencing of camera positions can be achieved if the camera is equipped with a GNSS receiver.

In the underwater realm, these tasks are significantly more challenging. The technologies employed in terrestrial surveys, such as laser electronic distance measurement and GNSS do not

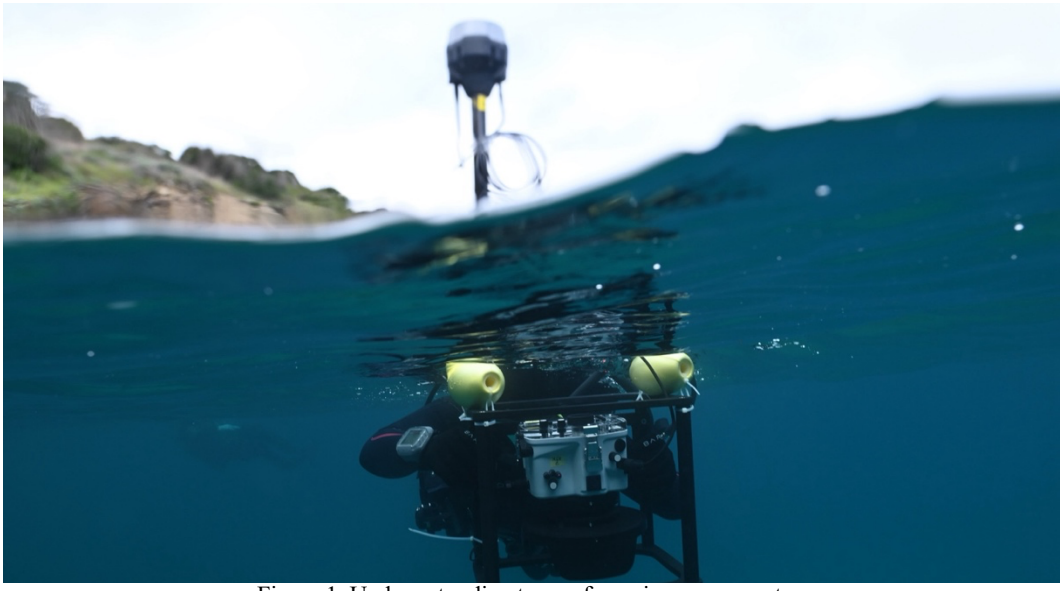

Figure 1. Underwater direct georeferencing camera setup

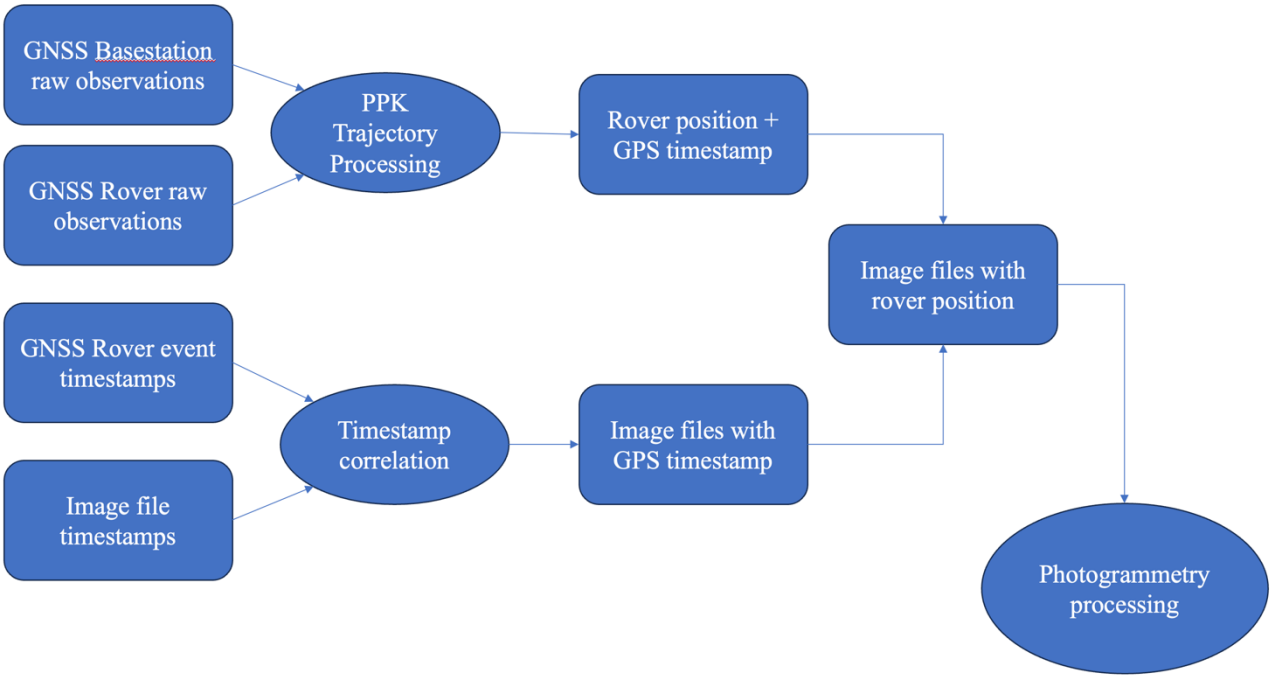

Figure 2. Software processing workflow

work underwater, and the difficulty for humans to work precisely underwater makes survey tasks challenging (Neyer et al., 2018). Underwater ground control points can be measured through a process of trilateration, which requires taking multiple redundant measurements between stations with a tape measure, with least squares adjustment of the observed measurements and statistical analysis to improve the confidence of the derived coordinates. Due to the time intensive nature of this survey technique, it cannot effectively be scaled up to larger areas (Skarlatos et al., 2017). Direct measurement of control point positions has also been demonstrated, using geodetic equipment adapted for underwater operations such as a tripod and multiple meters of extension poles to elevate a GNSS receiver above the surface of the water, but this technique is limited to shallow areas (Balletti et al., 2015, Wright, 2020). A similar concept for shallow water was demonstrated in Reich et al. (2021) using a prototype RTK buoy with an extensible rod for measuring ground control points underwater. Compared to GNSS receiver usage in terrestrial settings, the underwater setup is more cumbersome, and accuracy is reduced by potential deflection of the longer pole as well as induced motion from wave action and currents. In either of these cases, though it is possible to survey ground control underwater, it is significantly more laborious and time consuming than in a terrestrial context.

Another form of constraint can be provided through the measurement of the position of the images, as with the case of direct georeferencing for aerial photogrammetry. With the integration of GNSS receivers in many enterprise UAVs working with differential corrections, it is now possible to accurately record the position of the images to within a few centimeters. James et al. (2017) describes the use of such an approach to improve the accuracy of the estimated camera self-calibration parameters and the generated geometry without requiring ground control surveys. Morelli et al. (2022) describe a similar concept in a terrestrial context, integrating PPK (post processed kinematic) positioning of a GNSS receiver with a camera to avoid the necessity of deploying ground control points.

1.1 Underwater Direct Georeferencing

Given the challenges in deploying ground control points underwater, leveraging differential GNSS positioning as a constraint for an underwater photogrammetric camera system is attractive. As GNSS signals do not penetrate the water, the GNSS receiver must remain above water, while the camera should be submerged to avoid the additional complexity of imaging through the air-water interface at the sea surface (Chirayath and Earle, 2016). The rigid connection between the GNSS receiver and the camera means that the camera must be near the surface of the water, so this approach is applicable where visibility permits a camera at the surface to clearly resolve features on the seafloor. As with any multi-sensor setup, time synchronization must be considered to effectively leverage the two streams of data. Abadie et al. (2018) demonstrate 0.5 m accuracy compared to a multibeam sonar with this approach, synchronizing a mirrorless camera in an underwater enclosure with a GNSS receiver. Hatcher et al. (2020) present a more costly and complex sensor package supported by equipment on a boat, using multiple synchronized machine vision cameras in underwater housings combined with PPK GNSS positioning, with image exposures synchronized directly with the GNSS receiver. These data were evaluated through comparison with reference markers, scale bars, and repeated surveys, achieving 3 cm repeatability, which is in line with the expectation for such GNSS receivers. Jaud et al. (2023) demonstrate a lower cost approach, combining underwater GoPro images with RTK GNSS positioning data to provide photogrammetric constraints, with approximate frame synchronization of ~0.5 s. These data were collected in an intertidal zone and were compared with terrestrial photogrammetry with a mean error of 5 cm.

The objective of this contribution is to present the design of a self-contained system which leverages the underwater direct georeferencing approach to enable scalable capture of bathymetry in areas where features on the seafloor are clearly visible from the surface. The accuracy of the system is validated via comparisons with traditional underwater surveying

techniques in a controlled pool setting as well as in an uncontrolled near-shore field site by Catalina Island.

2. Methods

2.1 Photogrammetry

2.1.1 Equipment Setup

The core components of the system were a pair of survey grade GNSS receivers, and an underwater camera. One GNSS receiver was used as a stationary basestation nearby on land to provide corrections for the other GNSS receiver, “the rover”, attached to the camera setup. The raw observations from these receivers were processed with PPK to produce a trajectory for the GNSS rover, accurate to within a few centimeters. To be able to relate the rover trajectory with each of the images from the camera, two things were needed – time synchronization and a rigid mount. Time synchronization is critical to accurately associate the position of the GNSS rover with each image. This was achieved via a cable connecting the flash output of the camera with the event input on the GNSS rover, which records the timestamp of the image captures, allowing a one-to-one association of GNSS timestamps to images. To obtain the position of the camera from the GNSS rover position, a fixed, rigid lever arm offset was needed, which can be estimated as part of the image orientation process in a self-calibrating bundle adjustment. With these constraints applied, the images were then processed though the typical photogrammetric processing pipeline, with the creation of a dense point cloud, a digital surface model, and orthomosaic to represent the surveyed bathymetry. Figure 2 shows the data and processing workflow for this system.

The implementation of this setup consisted primarily of low-cost commercial off-the-shelf components to aid in the reproducibility of the setup. The underwater camera was a Nikon D780 with a 24 mm lens in an Ikelite housing with an 8 in dome port, and the GNSS receivers consisted of an Emlid Reach RS2+ for the basestation and an Emlid Reach RS3 for the rover. The cable for time synchronization was spliced together to connect the hotshoe with the RS3’s event input port, and a rigid frame provided a fixed mount between the camera, GNSS rover, and flotation (Figure 3).

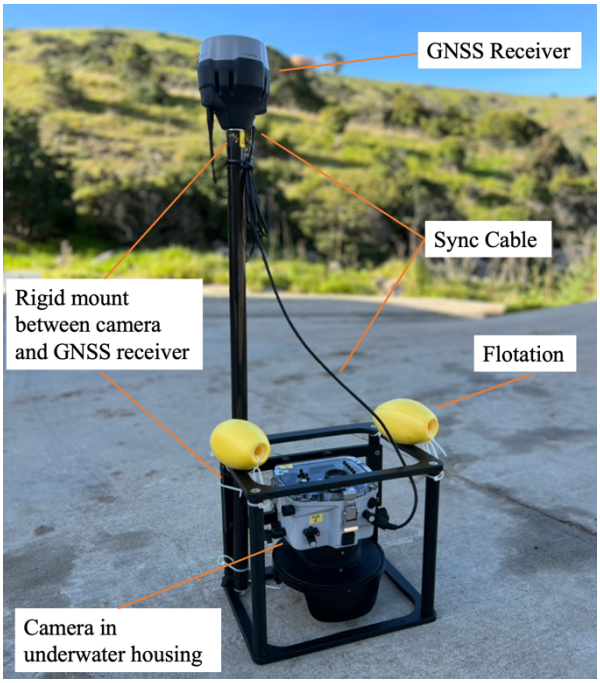

Figure 3. Components of the underwater direct georeferencing system

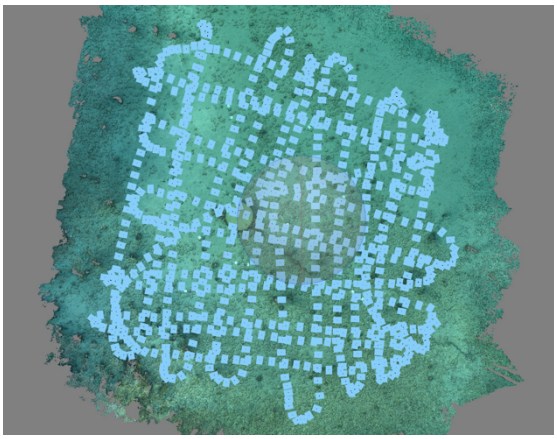

Figure 4. Double lawnmower acquisition pattern

2.1.2 Data Acquisition

The image acquisition strategy was analogous to that of a UAV, with a swimmer with a snorkel carrying the camera system through a double lawnmower pattern with the camera facing the nadir, targeting at least 75% forward overlap and sidelap. The camera was manually focused and autofocus was disabled. Image capture was set on the camera’s internal intervalometer to automatically trigger the image capture once per second, reducing the swimmer’s operating burden. As the GNSS receiver must remain above the water surface, the imaging distance was dictated by the depth of the seafloor below. This implies that altitude dependent parameters, such as GSD (ground sample distance), overlap, and sidelap may vary in a survey area. If the bathymetry in the area is known, a survey can be planned for the line spacing at the minimum depth, as targeting line spacing for the average depth will result in less overlap than predicted. For the 2-3 m depth of the pool, a 1m line spacing was targeted. For the shallow site in Catalina, with a depth of 4-6 m, a 2 m line spacing was targeted.

A complicating factor in the data acquisition process is the difficulty in executing the survey plan accurately in the water, as currents make it difficult to follow a straight line. This can be mitigated by decreasing line spacing to ensure that the minimum target overlaps are achieved despite these disturbances, but this reduces the efficiency of the survey.

2.1.3 Data Processing

The first step in processing was the PPK trajectory estimation. The RINEX files from the basestation and the rover were processed in Emlid Studio 1.7 to produce the trajectory of the rover’s antenna phase center (.pos file), as well as the interpolated points in the trajectory corresponding to the timestamps of the event triggers (_events.pos file). For local comparison, the trajectory was exported in a local cartesian East-North-Up coordinate frame with the basestation as the origin, but for georeferencing, the trajectory can also be exported in geographic Latitude-Longitude-Ellipsoid Height or ECEF (earth-centered earth frame) XYZ coordinates.

The second step was to correlate each image timestamp with the GNSS rover’s event timestamp. Since there was a hardwire connection between the camera hotshoe and the GNSS receiver’s

Figure 5. Underwater trilateration survey (left), underwater differential leveling (center), differential leveling laser mount (right)

event input, it was expected that the images and events will map one to one. However, occasionally GNSS event duplicates were observed, manifesting as two events within a 10 ms period, which must be discarded. Also, if any images were captured before the sync cable was connected with the GNSS rover, or the rover was unable to estimate its position while images were being captured (i.e. GNSS receiver entered a cave completely occluding satellite visibility), these extra images would also need to be discarded. In case the number of images was not equal to the number of event timestamps, this was be reconciled by noting that there should be a common time offset (neglecting clock drift) between corresponding image timestamps and event timestamps. By iteratively removing the extra image or event timestamps, a common time offset without discontinuities should be observed. Once this filtering process was completed and verified, the event trigger positions could be associated with the images one-to-one in time order.

To take advantage of the GNSS measurements, the photogrammetry software must be able to integrate the estimation of the lever arm offset between the antenna and camera centers into the bundle adjustment so it can relate the estimation of the camera position and orientation with the provided position of the GNSS trajectory, avoiding the need for an IMU to estimate the orientation. In Agisoft Metashape 2.0.2 (Agisoft, 2024), this was achieved by enabling adjustment of the GPS/INS offset. The images were loaded along with their corresponding GNSS positions, and the standard deviation of the GNSS position estimate was used in a weighted least squares approach. The typical photogrammetry processing workflow is then followed to generate a dense point cloud, DEM, and orthomosaic data products representing the bathymetry.

2.2 Underwater Geodetic Survey

The traditional approach to establishing ground control points in an underwater scene is to establish a geodetic network using trilateration and leveling. The approach employed largely follows the concepts in Rossi et al. (2019) and Nocerino et al. (2020). Reference points (RPs) were created using coded circular targets and weighted down to sit on the seafloor. Two types of RPs were used – scale bars with 2 coded circular targets rigidly fixed 50 cm apart with only one target considered for the geodetic survey, and single circular targets which were placed on an elevated assembly to create additional vertical variation in the RP coordinates. The geodetic survey consisted of 2 stages: the trilateration survey and the differential leveling survey.

For the trilateration survey, the distances between pairs of RPs and their inverses were measured with a fiberglass tape measure. For the differential leveling, a new adapter was designed to mount a commercially available underwater green laser pointer onto a tribrach for leveling, allowing for rotation about the vertical axis so the laser point could be projected in the horizontal plane. As the optical axis of the laser may not be parallel to the housing, the adapter was designed symmetrically to allow it to be quickly mounted upside down, so errors in misalignment of the optical axis can be averaged out. To perform the measurement, one diver set the tripod in the midpoint between markers to be measured, and leveled the tribrach, while the other diver placed the stadia rod vertically on the RP to be measured. The first diver then turned the laser to point to the stadia rod, and the second diver recorded the value. Once the first value was recorded, the laser adapter was inverted, again pointed towards the stadia rod, and the second value was recorded. This process was repeated for the second target, and for each pair of targets in the network. Inverting the laser pointer about its axis cancels out inclination error of the laser if the tripod is placed in the midpoint of the two markers to be measured, though residual leveling errors from the sensitivity limits of the bubble level (8 arcminutes in this setup) are expected to be less than 1 cm for lines shorter than 5 m.

The data from these surveys were adjusted using GNU Gama (Cepek, 2002), an open-source software for geodetic network adjustment that uses the weighted least squares method. The network was adjusted in a free network combining slant distance and height difference observations. The estimated a priori standard deviations of the observations were 3 mm and 4 mm, for the slant distance and for the height differences, respectively. The average estimated precisions resulting from the free network adjustment in Gama were σ_{XY} = 5 mm σ_Z= 8 mm.

2.3 RTK GNSS Pole

Another approach to measure the coordinates of the underwater targets was by directly measuring their positions using a tilt-compensated RTK GNSS receiver with extended lengths of survey rod in order to keep the GNSS receiver above the water surface, while the other end of the pole could reach the underwater targets. The tilt compensation feature allows the coordinates of the tip of the survey rod to be determined without requiring the survey rod to be entirely plumb, which would be a cumbersome task for such a long survey rod underwater.

The equipment used was an Emlid Reach RS3 receiver with up to 7 m of survey rod length, corrected against an Emlid Reach RS2+ which was set up as a static basestation nearby (within 300 m). RTK positioning precision for the RS3 is specified as 7 mm + 1 ppm horizontal, and 14 mm + 1 ppm vertical, with an additional error from the usage of tilt compensation of 2 mm + 0.3 mm/degree. Since the basestation is positioned within 1 km, the ppm terms can be neglected as < 1 mm. An expected tilt angle of 20 deg yields a tilt error of 8 mm, for overall expected instrument precision of 15 mm horizontal, 14 mm vertical.

To deploy the equipment, the survey rod was assembled on shore, then carried by the divers to the site. As the survey rod is hollow, water was allowed to flood the lower segments of the rod to make

it closer to being neutrally buoyant. To record each point, a diver on the bottom held the point of the survey rod on the RP, while another diver stabilized the rod, and a surface swimmer attempted to maintain the rod roughly level. On the surface, a smartphone in a waterproof pouch was connected to the RS3 receiver via Wi-Fi, and the Emlid Flow app was used to name and record each point. Each RP was measured 4 times with 2 seconds in between to increase confidence in the measurement.

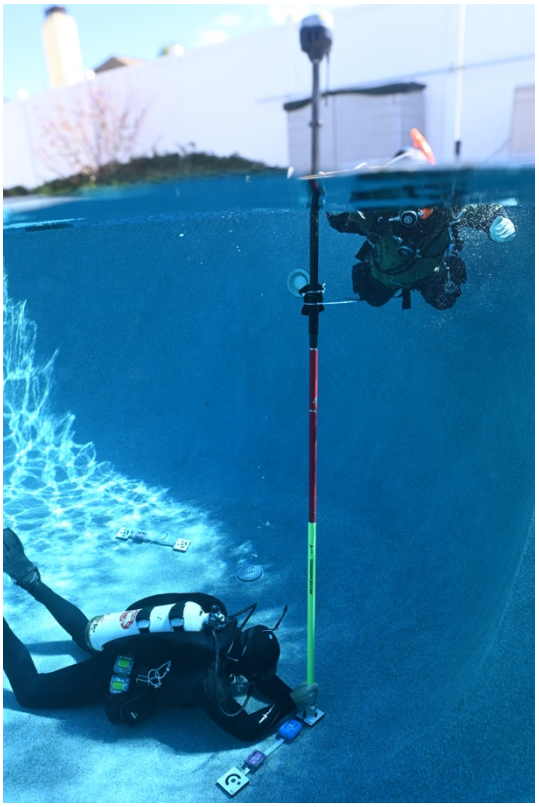

Figure 6. RTK pole measuring RP in pool test

3. Results

The accuracy of this photogrammetry system is demonstrated in real world tests through comparison with traditional techniques. First, the system is demonstrated in an outdoor pool to validate expected accuracy in a controlled environment with perfect visibility conditions. For local accuracy evaluation, scale bars are placed throughout the scene. A local geodetic network is established through trilateration and leveling, and positions are compared. Additionally, the same reference points are directly measured with a tilt compensated GNSS receiver and a long pole. The comparisons between the direct georeferencing approach and the traditional survey techniques are expected to be consistent within a few centimeters. Second, a near-shore field test site in the ocean with varied bathymetry and favorable visibility is established. The study area consists of a 10 m x 10 m plot with depths of approximately 3-5 m. The maximum water visibility was greater than the water depth, as the targets were clearly visible from the surface. The same traditional validation techniques are employed as in the pool test, with installation of scale bars and reference points measured both via trilateration and with the tilt compensated GNSS receiver. Finally, an additional test site with a depth of approximately 10 m is captured and validated with scale bars, demonstrating the intended application of this system for scalable bathymetric survey in deeper areas without the necessity for ground control.

3.1 Pool Tests

An initial set of testing was conducted in an outdoor pool to train for the survey techniques, and to establish a baseline comparison of measurements in a controlled setting. The pool dimensions were 5 m x 10 meters, with a depth ranging from 1-3 m. Eight scale bars were weighted down and placed around the pool, and one target from each scale bar was chosen to be used in the geodetic survey and the RTK pole survey. The geodetic survey coordinates adjusted in Gama achieved an average standard deviation of 3.3 mm in X, 3.3 mm in Y and 2.0 mm in Z. The RTK pole survey used a 2.8 m pole, and achieved an average standard deviation of 5 mm in X, 7 mm in Y and 9 mm in Z. The photogrammetry survey achieved a GSD of 0.3 mm and an $RMSE_{XYZ}$ of 2.4 cm between the GNSS positions provided for the images and the adjusted positions from bundle adjustment.

Accuracy was assessed as residuals of a 3D rigid similarity transformation with the scale factor computed between the photogrammetrically derived marker coordinates and those obtained from the RTK pole and geodetic survey, respectively. These results are reported in Table 1 and indicate agreement between the three measurement techniques of better than 2 cm.

	$RMSE_X$ [mm]	$RMSE_Y$ [mm]	$RMSE_Z$ [mm]	$RMSE_{XYZ}$ [mm]
RTK Pole	5.9	10.9	6.6	14.0
Geodetic survey	6.0	5.5	1.2	8.2

Table 1. Residuals for the similarity transformation between RPs measured with photogrammetry and RTK pole or geodetic survey in the pool test

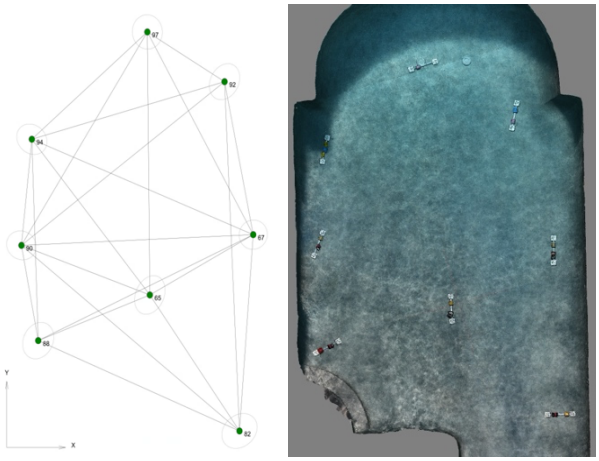

Figure 7. Adjusted geodetic network (left), orthophoto of pool test (right)

3.2 Catalina Shallow Site

The primary testing site was established in a near-shore environment by Catalina Island, in a roughly 10 m x 10 m area with depths ranging from 4-6 m. Seven scale bars and three individual markers were weighted down and installed in the site. Three survey techniques were employed to measure the positions of the markers in the site: geodetic survey, RTK pole, and photogrammetry.

The geodetic survey of the ten markers was completed over two dives totaling 150 min underwater. The first dive to complete the differential leveling measurements took 82 min, and the second dive to complete the trilateration measurements took 68 min. The geodetic survey coordinates adjusted in Gama achieved an average standard deviation of 1.5 mm in X, 1.4 mm in Y, and 1.9 mm in Z.

The RTK pole survey was completed in 10 min. Due to the increased depth of this site compared to the pool, the pole length was increased to 7 m. While repeating the four measurements for each marker, decimeter level variations were observed between the coordinates on each marker, and visible deflection of the pole was observed, likely due to a combination of current and the divers attempting to keep the pole vertical. Figure 8 shows the scattered distribution of the resulting measured points, overlaid on top of an orthophoto mosaic. From averaging the four measurements of each marker in the RTK survey, an average standard deviation of 78 mm in X, 85 mm in Y, and 17 mm in Z was observed. The results of the comparison with the photogrammetric data are reported in Table 2, but as the residuals are in the decimeter scale, they cannot be used to validate the accuracy of the photogrammetric model.

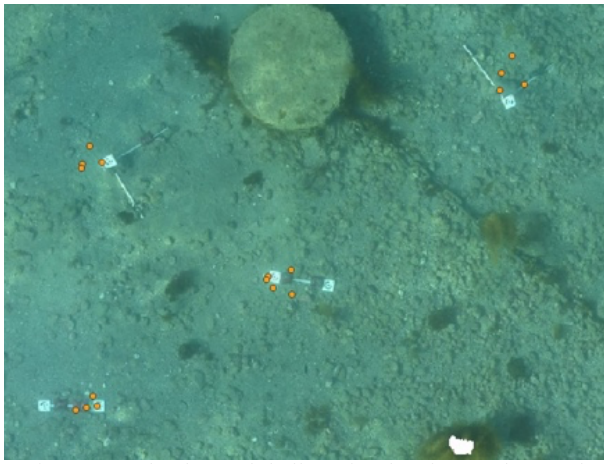

Figure 8. Orthophoto of shallow site showing markers and RTK pole measurement scatter

	$RMSE_X$ [mm]	$RMSE_Y$ [mm]	$RMSE_Z$ [mm]	$RMSE_{XYZ}$ [mm]
shallow	73	107	29	133

Table 2. Residuals of the similarity transformation without scale factor between RPs measured with RTK (averaged) and underwater geodetic surveying.

Five photogrammetry surveys were conducted in the shallow site, with an average GSD of 1 mm to demonstrate the consistency of the results, particularly with different GNSS satellite constellations and varied water clarity through the day. The surveys were spread over 3 days, with 3 of the surveys (shallow2, shallow3, shallow4) being conducted on the same day as the geodetic survey and RTK pole survey to mitigate against the possibility of the temporarily installed RPs moving due to tidal flushing or other disturbances. A summary of the photogrammetry survey statistics is presented in Table 3. The camera centers RMSE is the root mean square of the residuals between the estimated camera positions from the bundle adjustment solution and the PPK positions of the GNSS antenna, where the lever arm is estimated within the bundle adjustment.

Survey name	Survey time of day	Survey length (min)	RMSE camera centers [mm]	# images
shallow1	17:12	22	24.8	1290
shallow2	10:31	20	21.9	1225
shallow3	13:28	17	21.9	1021
shallow4	16:43	14	23.5	829
shallow5	9:08	17	25.9	1024

Table 3. Summary of photogrammetry acquisitions in shallow site

3.2.1 Accuracy Assessment of RPs

The geometric accuracy of the photogrammetric reconstructions was evaluated though comparison with the coordinates of the RPs obtained from the underwater geodetic survey. The photogrammetric reconstruction was obtained using the PPK positions of the GNSS antenna mounted on the underwater camera system with their estimated precision as known coordinates in the bundle adjustment, with consideration for the lever arm between the camera and the antenna. The results, shown in Table 4, represent the RMS residuals of a similarity transformation without scale factor between RPs triangulated by photogrammetry and the adjusted coordinates from the underwater geodetic surveying. One of the markers was visibly displaced between the shallow1 acquisition and the geodetic network survey the following day, so that marker was not constrained in the comparison for the shallow1 dataset.

Survey	$RMSE_X$ [mm]	$RMSE_Y$ [mm]	$RMSE_Z$ [mm]	$RMSE_{XYZ}$ [mm]
shallow1	6	3	3	7
shallow2	8	5	2	9
shallow3	5	3	3	7
shallow4	8	4	2	10
shallow5	4	4	3	6

Table 4. Residuals of the similarity transformation without scale factor between RPs measured with the underwater photogrammetry system featuring a GNSS antenna above the water and the underwater geodetic surveying.

3.2.2 Assessment of Length Measurement Error on Scale Bars

To evaluate the attainable accuracy in scaling of the photogrammetric reconstruction, the values of the seven 50 cm long scale bars throughout the scene were measured, shown in Table 5. The scalebar residuals are on the order of a millimeter, of the same order as the GSD achieved in this site.

Survey	mean scalebar error [mm]	stdev [mm]
shallow1	0.6	0.8
shallow2	1.0	1.1
shallow3	0.5	0.8
shallow4	1.2	1.1
shallow5	-0.2	0.5

Table 5. Residuals of the scale bars as measured in the photogrammetry surveys compared to known reference lengths

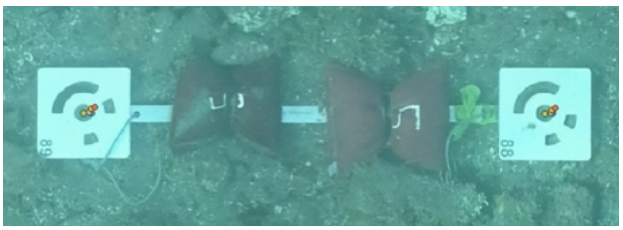

Figure 9. 0.5m scale bar with markers plotted for each of the 5 shallow surveys

3.2.3 Georeferencing Repeatability

Georeferencing repeatability was assessed by comparing the marker positions between the five photogrammetric reconstructions, using only the GNSS trajectory as constraint. Planimetric consistency was observed to be at the sub centimeter level, and vertical consistency was observed to be sub centimeter for shallow2, shallow3, and shallow4, with 2-3 cm vertical shifts between shallow1 and shallow2, as well as shallow4 to shallow5. These results, shown visually in Figure 10, are consistent with the expectation for RTK GNSS.

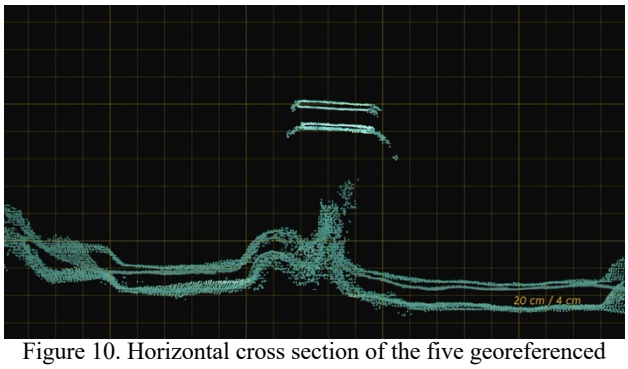

Figure 10. Horizontal cross section of the five georeferenced photogrammetry surveys showing vertical shifts

3.3 Catalina Deep Site

A second test site was established in an area with up to 10 m in depth to test the limitations of the system with depth and visibility. Seven scale bars and three markers were installed in the 10 m x 10 m area of the site. In this site, three photogrammetry surveys were conducted in an expanded area including the core 10 m x 10 m site where the markers were installed. The first survey was similar to those conducted in the shallow site, with the snorkeler swimming a double lawnmower pattern over a 25 m x 20 m area. The second survey was attaching the camera system to a kayak and paddling a 70 m x 15 m area. The third survey was with a snorkeler swimming a double lawnmower in a 50 m x 20 m area.

Survey name	Survey time of day	Survey length (min)	Survey area	RMSE cam center [mm]	# images
deep1	11:26	26	25m x 20m	20.4	1590
deep2	13:14	40	70m x 15m	20.3	2437
deep3	16:04	34	50m x 20m	18.8	2237

Table 6. Summary of photogrammetry acquisitions in deep site

Of the three datasets, the deep1 acquisition had the worst visibility, though it was estimated to be greater than 1 Secchi depth, as the high contrast of the RPs was still visible in the images. However, features on the sandy bottom of the seafloor were not clearly distinguishable, and images over the area of lower visibility failed to align, likely a result of failed feature detection. In the deep2 and deep3 datasets, visibility continued to improve, and the majority of images in the same area were able to be aligned. This suggests that the guideline for applicability of this sensing technique should be visibility beyond 1 Secchi depth, with some dependence on how easily the features are obscured by reduced visibility (i.e. small sand ripples would be obscured more easily than large coral formations).

4. Conclusions

This paper reports our experiences of georeferencing an underwater photogrammetric survey in shallow clear water. Several tests in a controlled environment, a pool, along with open water settings are discussed. We compared different approaches: setting up an underwater geodetic network through trilateration and leveling, RTK GNSS measurements with a tilt-compensated pole, and direct georeferencing of the underwater camera positions with a PPK GNSS receiver rigidly attached to the camera itself. The tests were carried out with very short baselines between the GNSS reference basestation and the rover. The results show that integrating PPK GNSS measurements into the photogrammetric workflow proves to be an effective approach for georeferencing of underwater surveys, providing sub centimeter geometric accuracy when compared to underwater geodetic network. We can then observe that this method is promising for monitoring applications based on the analysis of orthophotos, thanks to the sub centimeter planimetric georeferencing repeatability. Further investigations are necessary to reduce the observed vertical shifts. Although the shifts fall within the expected performance of the method, they may negatively impact the comparison between 3D surface models.

The tilt-compensated RTK GNSS measurements did not perform within the required accuracy for monitoring purposes when sub centimetric changes are expected.

Acknowledgements

This research was supported in part by the USACE Engineer Research and Development Center Cooperative Agreement W9132T-22-2-0014, the National Science Foundation under award #CNS-1338192, MRI: Development of Advanced Visualization Instrumentation for the Collaborative Exploration of Big Data, ALERTCalifornia: Developing Technology to Stay Ahead of Disasters, the Center for Environmental Imaging, the Kinsella Expedition Fund, as well as the Young Researcher Mobility Programme (MGR) Finanziamento Legge regionale 7 agosto 2007, n. 7 “Promozione della Ricerca Scientifica e dell’Innovazione Tecnologica in Sardegna,” and programma attività annualità 2022 through the project “GATE: La GeomaticA per il paTrimonio sommErso”, the POSEIDON - multitemPOral SEagrass mapping and monitoring of posIDONia meadows and banquettes for blue carbon conservation (E53D23021870001), a research project of Italian national relevance initiative “Italia Domani - Piano Nazionale di Ripresa e Resilienza” (PNRR) funded by the European Commission - Next Generation EU. We also thank the USC Wrigley Marine Science Center for hosting our experiments and our dive team, including Rich Walsh and Brian Zgliczynski. Opinions, findings,

and conclusions from this study are those of the authors, and do not necessarily reflect the opinions of the research sponsors.

References

Abadie, A., Boissery, P. and Viala, C., 2018. Georeferenced underwater photogrammetry to map marine habitats and submerged artificial structures. The Photogrammetric Record, 33(164), pp.448-469.

Agisoft, 2024. Metashape Professional, Version 2.0.2. https://www.agisoft.com/downloads/installer/ (25 August 2023)

Balletti, C., Beltrame, C., Costa, E., Guerra, F. and Vernier, P., 2015. Underwater photogrammetry and 3D reconstruction of marble cargos shipwreck. The International Archives of the photogrammetry, remote sensing and spatial information sciences, 40, pp.7-13.

Čepek, A., 2002. The GNU Gama project-adjustment of geodetic networks. Acta Polytechnica, 42(3).

Chirayath, V., Earle, S.A., 2016. Drones that see through waves – preliminary results from airborne fluid lensing for centimetre-scale aquatic conservation. Aquatic Conservation: Marine and Freshwater Ecosystems 26, 237–250. doi:10.1002/aqc.2654

Hatcher, G.A., Warrick, J.A., Ritchie, A.C., Dailey, E.T., Zawada, D.G., Kranenburg, C., Yates, K.K., 2020. Accurate bathymetric maps from underwater digital imagery without ground control. Frontiers in Marine Science 7. doi:10.3389/fmars.2020.00525

James, M.R., Robson, S., 2014. Mitigating systematic error in topographic models derived from UAV and ground-based image networks. Earth Surface Processes and Landforms 39, 1413–1420. doi:10.1002/esp.3609

James, M.R., Robson, S., Smith, M.W., 2017. 3-D uncertainty-based topographic change detection with structure-from-motion photogrammetry: Precision maps for ground control and directly georeferenced surveys. Earth Surface Processes and Landforms 42, 1769–1788. doi:10.1002/esp.4125

Jaud, M., Delsol, S., Urbina-Barreto, I., Augereau, E., Cordier, E., Guilhaumon, F., Le Dantec, N., Floc’h, F., Delacourt, C., 2023. Low-tech and low-cost system for high-resolution underwater RTK photogrammetry in coastal shallow waters. Remote Sensing 16, 20. doi:10.3390/rs16010020

Morelli, L., Menna, F., Vitti, A., Remondino, F., 2022. Action cams and low-cost multi-frequency antennas for GNSS assisted photogrammetric applications without ground control points. The International Archives of the Photogrammetry, Remote Sensing and Spatial Information Sciences XLVIII-2/W1-2022, 171–176. doi:10.5194/isprs-archives-xlviii-2-w1-2022-171-2022

Neyer, F., Nocerino, E., Gruen, A., 2018. Monitoring coral growth – the dichotomy between underwater photogrammetry and Geodetic Control Network. The International Archives of the Photogrammetry, Remote Sensing and Spatial Information Sciences XLII–2, 759–766. doi:10.5194/isprs-archives-xlii-2-759-2018

Nocerino, E., Menna, F., Gruen, A., Troyer, M., Capra, A., Castagnetti, C., Rossi, P., Brooks, A.J., Schmitt, R.J. and Holbrook, S.J., 2020. Coral reef monitoring by scuba divers using underwater photogrammetry and geodetic surveying. Remote Sensing, 12(18), p.3036.

Nocerino, E., Menna, F. and Remondino, F., 2014. Accuracy of typical photogrammetric networks in cultural heritage 3D modeling projects. The international archives of the photogrammetry, remote sensing and spatial information sciences, 40, pp.465-472.

Reich, J., Steiner, P., Ballmer, A., Emmenegger, L., Hostettler, M., Stäheli, C., Naumov, G., Taneski, B., Todoroska, V., Schindler, K. and Hafner, A., 2021. A novel structure from motion-based approach to underwater pile field documentation. Journal of Archaeological Science: Reports, 39, p.103120.

Rossi, P., Castagnetti, C., Capra, A., Brooks, A.J., Mancini, F., 2019. Detecting change in Coral Reef 3D structure using underwater photogrammetry: Critical Issues and Performance Metrics. Applied Geomatics 12, 3–17. doi:10.1007/s12518-019-00263-w

Skarlatos, D., Agrafiotis, P., Menna, F., Nocerino, E., Remondino, F., 2017: Ground control networks for underwater photogrammetry in archaeological excavations. In Proceedings of the 3rd IMEKO International Conference on Metrology for Archaeology and Cultural Heritage, MetroArcheo 2017. October 23-25, 2017, Lecce, Italy

Wright, A.E., Conlin, D.L., Shope, S.M., 2020. Assessing the accuracy of underwater photogrammetry for archaeology: A comparison of structure from motion photogrammetry and real time kinematic survey at the East Key Construction Wreck. Journal of Marine Science and Engineering 8, 849. doi:10.3390/jmse8110849